Ruxolitinib-induced defects in DNA repair cause sensitivity to PARP inhibitors in myeloproliferative neoplasms

Short title: JAK1/2 and PARP inhibitors against MPNs

Margaret Nieborowska-Skorska[1], Silvia Maifrede[1], Yashodhara Dasgupta[1], Katherine Sullivan[1], Sylwia Flis[1,2], Bac Viet Le[1,3], Martyna Solecka[1], Elizaveta A. Belyaeva[4], Lucia Kubovcakova[5], Morgan Nawrocki[1], Martin Kirschner[6], Huaqing Zhao[7], Josef T. Prchal[8], Katarzyna Piwocka[3], Alison R. Moliterno[9], Mariusz Wasik[4], Steffen Koschmieder[6], Tony R. Green[10], Radek C. Skoda[5], and Tomasz Skorski[1,*]

[1]Temple University School of Medicine, Department of Microbiology and Immunology and Fels Institute for Cancer Research & Molecular Biology, Philadelphia, PA, 19140, USA

[2]National Medicines Institute, Department of Pharmacology, Warsaw, 00-725, Poland

[3]Nencki Institute of Experimental Biology, Laboratory of Cytometry, Warsaw, 02-093, Poland

[4]Department of Pathology and Laboratory Medicine, University of Pennsylvania, Philadelphia, PA 19102, USA

[5]University Hospital Basel and University of Basel, Department of Biomedicine, 4031 Basel, Switzerland

[6]RWTH Aachen University, Department of Hematology, Oncology, Hemostaseology, and Stem Cell Transplantation, Faculty of Medicine, Aachen, Germany.

[7]Temple University Lewis Katz School of Medicine, Department of Clinical Sciences, Philadelphia, PA, 19140, USA

[8]University of Utah School of Medicine, Salt Lake City, UT 84132 USA

[9]Division of Hematology, Department of Medicine, The Johns Hopkins University School of Medicine, Baltimore, MD, USA

[10]Wellcome Trust-MRC Cambridge Stem Cell Institute, Cambridge Institute for Medical Research and Department of Haematology, University of Cambridge, Cambridge, UK

Corresponding author:
Tomasz Skorski, Temple University, School of Medicine, Department of Microbiology and Immunology and Fels Institute for Cancer Research and Molecular Biology 3400 N. Broad

Street, MRB 548, Philadelphia, PA 19140, USA, Phone: 215-707-9157, Fax: 215-707-9160
email: tskorski@temple.edu

Word counts: Abstract- 176; Text –3,393; Figures – 6; References – 60.

Scientific Category – Myeloid Neoplasia

KEY POINTS:

- Ruxolitinib caused DNA repair defects and sensitized MPN stem and progenitor cells to PARP inhibitors.
- Quiescent and proliferating MPN cells were eliminated by ruxolitinib and olaparib +/- hydroxyurea.

Abstract

Myeloproliferative neoplasms (MPNs) often carry JAK2(V617F), MPL(W515L), or CALR(del52) mutations. Current treatment options for MPNs include cytoreduction by hydroxyurea and JAK1/2 inhibition by ruxolitinib, both of which are not curative. We show here that cell lines expressing JAK2(V617F), MPL(W515L) or CALR(del52) accumulated reactive oxygen species-induced DNA double-strand breaks (DSBs) and were modestly sensitive to poly-ADP-ribose polymerase (PARP) inhibitors olaparib and BMN673. At the same time primary MPN cell samples from individual patients displayed a high degree of variability in the sensitivity to these drugs. Ruxolitinib inhibited two major DSB repair mechanisms, BRCA-mediated homologous recombination and DNA-PK –mediated non-homologous end-joining and, when combined with olaparib, caused abundant accumulation of toxic DSBs resulting in enhanced elimination of MPN primary cells, including the disease-initiating cells from the majority of patients. Moreover, the combination of BMN673, ruxolitinib and hydroxyurea was highly effective in vivo against JAK2(V617F)-positive murine MPN-like disease and also against JAK2(V617F), CALR(del52), and MPL(W515L)-positive primary MPN xenografts. In conclusion, we postulate that ruxolitinib-induced deficiencies in DSB repair pathways sensitized MPN cells to synthetic lethality triggered by PARP inhibitors.

Introduction

Philadelphia chromosome-negative (Ph-) myeloproliferative neoplasms (MPNs) include polycythemia vera (PV), essential thrombocythemia (ET) and primary myelofibrosis (PMF), which are associated with mutations in *JAK2*, *CALR* and *MPL* genes [1,2]. Current treatment options for Ph- MPNs include cytoreductive therapy with hydroxyurea, and the JAK1/2 inhibitor (JAK1/2i) ruxolitinib, which produce durable reductions in splenomegaly and improvement of symptoms and probably of survival, but do not eliminate the disease-initiating cell population [3,4]. MPNs usually present in chronic phase, but they may eventually accelerate and transform into secondary acute myeloid leukemia which carries a dismal prognosis and is always fatal [5]. Therefore, it is imperative to generate new therapies, which alone or in combination with conventional treatments induce long-term remission, even in patients who have progressed to the acute leukemia stage. The combination of agents which target different mechanisms promises to provide a successful rational future strategy [6].

MPN cells contain elevated levels of reactive oxygen species (ROS) and stalled replication forks, resulting in accumulation of high numbers of toxic DNA double-strand breaks (DSBs) [7-12]. Therefore, we reasoned that MPN cell survival may depend on DSB repair mechanisms [13-21]. DSBs are repaired by two major mechanisms, BRCA1/2-mediated homologous recombination repair (HRR) and DNA-PKcs-mediated non-homologous end-joining (D-NHEJ) [22]. In addition, poly-ADP-ribose polymerase 1 (PARP1) plays a central role in preventing/repairing lethal DSBs by activation of base excision repair/single-stranded DNA break repair, by stimulation of fork repair/restart, and by mediating the back-up NHEJ (B-NHEJ) repair [23-26].

Accumulation of potentially lethal DSBs in MPN cells could create an opportunity to eliminate these cells by targeting DNA repair mechanisms. Here, we tested the hypothesis that combination of ruxolitinib-mediated inhibition of DSB repair with a PARP inhibitor (PARPi)

and/or hydroxyurea causes accumulation of lethal DSBs beyond reparable thresholds resulting in enhanced elimination of MPN cells.

Materials and Methods

Primary cells

Peripheral blood and bone marrow samples from patients with newly diagnosed MPNs (Supplementary Table 1) were obtained from: (1) Department of Biomedicine, Basel University, Switzerland, (2) Department of Internal Medicine, Hematology and Oncology, Medical University, Aachen, Germany, (3) Department of Hematology, University of Cambridge, UK, and (4) Myeloproliferative Disorders Clinic, Huntsman Cancer Hospital, Salt Lake City, UT, USA. Samples of normal hematopoietic cells were purchased from Cambrex Bio Science (Walkersville, MD, USA). Lin^-CD34^+ cells were obtained from mononuclear fractions by magnetic sorting using the EasySep negative selection human progenitor cell enrichment cocktail followed by human CD34 positive selection cocktail (StemCell Technologies) as described before [27].

Cell lines

BaF3-JAK2(V617F)+EpoR, 32Dcl3-MPL(W515L), 32Dcl3-CALR(del52)+MPL(wt) cell lines, and their BaF3-EpoR and 32Dcl3-MPL(wt) parental counterparts were described before [28-30]. BaF3-HR2 and Jak2(V617F)-positive BaF3-HR2 cells carrying genome-integrated HR-EGFP cassette were generously provided by Dr W. Vainchenker [31]. They were cultivated in IMDM supplemented with 10% FBS, IL-3+Epo, and antibiotic cocktail.

Inhibitors/drugs

The following compounds were used: JAK1/2 inhibitor ruxolitinib (Selleckchem), PARP inhibitors BMN673 and olaparib (Selleckchem), mutT homologue 1 (MTH1) Inhibitor SCH51344 (Tocris),

ROS scavenger vitamin E (Sigma), and ribonucleoside diphosphate reductase inhibitor hydroxyurea (Selleckchem).

Western analyses

Nuclear cell lysates and total cell lysates were obtained and resolved by SDS-PAGE electrophoresis as previously described [27]. Protein expressions were analyzed using primary antibodies detecting: BRCA1 (#MAB22101, R&D Systems), BRCA2 (#MAB2476, R&D Systems), RAD51 (#sc6862, Santa Cruz Biotech.), DNA-PKcs (#A300-518A, Bethyl Lab.), Ku70 (#A302-623A, Bethyl Lab.), Ku80 (#MA5-15873, ThermoFisher Scientific), PARP1 (#sc7150, Santa Cruz Biotech), PALB2 (#A302-627A, Bethyl Lab.), Lig3 (#GTX70147, GeneTex), Lig4 (#ab26039, Abcam), STAT5 (#SC-28685, Santa Cruz), phospho-STAT5A (Ser780) (#sc-101805, Santa Cruz), cleaved caspase-3 (#9661, Cell Signaling), lamin B (#sc-6216, Santa Cruz), and beta-actin (#A5316, Sigma).

Examination of DSB repairs

Cells were cultured in IMDM supplemented with 10% FBS, IL-3 and Epo in the presence or absence of 0.15 μM roxulitinib. HRR events were measured as described before with modification [32]. Five million JAK2(V617F)-positive Ba/F3-HR2 cells carrying HR-EGFP cassette were nucleofected with 5 μg of pCBASCE1 and 2.5 μg of pDsRED-Mito plasmids using Nucleofector (Lonza; program U-008, Human CD34 Cell Nucleofector® Kit). Expression of I-*Sce*I causes a DSB in the specific restriction site included in the HR-EGFP cassette, and pDsRed1-Mito encodes red fluorescent protein with a mitochondrial localization signal to control the efficiency of transfection. HRR event restores functional EGFP expression, which is readily detected by fluorescent microscope 48h after transfection with I-*Sce*I. After 72 hours, cells were analyzed by flow cytometry for the percentage of GFP+ cells to assess HRR activity. D-NHEJ was measured in cell-free extracts as described before with modification [32]. Briefly, 200ng of the substrate plasmid (pBluescript KS+ linear plasmids digested XhoI+XbaI to generate non-

compatible 5' overhangs) was added to the reaction mix containing 10 μg nuclear lysate and incubated for 1h at 37°C. Products of D-NHEJ reaction were resolved in 0.5% agarose gel containing 0.5μg/ml of ethidium bromide, scanned with Adobe Photoshop and analyzed by ImageQuant TL (Amersham Bioscience, Piscataway, NJ, USA).

I*n vitro* treatment

Cells were cultivated in IMDM supplemented with 10% FBS and growth factors [100 ng/ml SCF; 10 ng/ml Flt3 ligand; 20 ng/ml IL-3, IL-6, G-CSF and GM-CSF; 12 units/ml EPO; 2.5 ng/ml TPO]. Ruxolitinib, hydroxyurea, vitamin E, SCH51344, olaparib and/or BMN673 were added for 3-5 days followed by trypan blue exclusion counting and/or plating in methylcellulose in the presence of growth factors. Colonies were counted after 7-10 days. For quiescent/proliferating cells, Lin^- cells were stained with cell trace violet (CTV) (eBioscience) and incubated for 5 days in StemSpan®SFEM medium (Stem Cell Technologies, Vancouver, Canada) supplemented with the cocktail of growth factors (see above) and inhibitors when indicated. Quiescent (CTV^{max}) and proliferating (CTV^{low}) leukemia cells were detected by flow cytometry using fluorochrome-conjugated anti-Lin (#340546), anti-CD34 (#347203) and anti-CD38 (#555460) antibodies (all from BD Biosciences) as described before [33].

GFP+JAK2(V671F) murine MPN-like disease

C57BL/6 recipient mice (The Jackson Laboratories) were subjected to 900 Gy total body irradiation followed by i.v. injection of 1:1 mixture of 10^6 GFP+JAK2(V671F) and 10^6 wild-type bone marrow cells as described before [3]. Five weeks later mice were treated with vehicle, hydroxyurea (30 mg/kg BID i.p.), ruxolitinib (30 mg/kg BID by oral gavage), BMN673 (0.33 mg/kg i.v.), and combinations of these drugs for 3 weeks. GFP+JAK2(V617F) cells were examined among total bone marrow cells, splenocytes and peripheral blood leukocytes at the end of treatment; in addition a fraction of GFP+JAK2(V617F) $Lin^-Sca1^+c\text{-}Kit^+$ cells was assessed in the bone marrow population.

Primary MPN xenografts

NOD.*Rag1*$^{-/-}$;*γc*^{null} mice expressing human IL-3, GM-CSF and SCF (NRGS mice [34], The Jackson Laboratories) were sub-lethally irradiated (600 Gy) and injected with 1 x 10^6 Lin^-CD34^+ primary MPN cells expressing JAK2(V617F), CALR(del52) or MPL(W515L). Three weeks later mice were treated as described above with vehicle, hydroxyurea + ruxolitinib, BMN673, and hydroxyurea + ruxolitinib + BMN673 for 3 weeks. Human $CD45^+$ ($hCD45^+$) cells, $hCD45^+Lin^-CD34^+$ MPN progenitors and stem cell-enriched $hCD45^+Lin^-CD34^+CD38^-$ MPN cells were detected in bone marrow cells, splenocytes and/or peripheral blood leukocytes at the end of treatment as described before [33].

Statistical analyses

Data are presented as mean ± standard deviation (SD) from three independent experiments and were compared using the unpaired two-tailed Student t test; p values less than 0.05 were considered significant. The response additivity approach was used to study the synergistic effects [35]. This approach shows a positive drug combination effect when the observed combination effect is greater than the expected additive effect by the sum of the individual effects. The p-value for the possible synergistic effect is given by the significance of the interaction effect in a factorial analysis of variance of the individual and combination effects.

Study Approval

Studies involving human samples were approved by the Temple University Institutional Review Board and met all requirements of the Declaration of Helsinki. Animal studies were approved by the Temple University Institutional Animal Care and Use Committee.

Results

Wide-range sensitivity of MPN cells to PARP inhibitors

Murine cell lines expressing JAK2(V617F)+EpoR, MPL(W515L), and CALR(del52)+MPL(wt) displayed modestly increased (by 20-40%), but statistically significant ($p \leq 0.002$) sensitivity to PARP inhibitors olaparib and BMN673 when compared to non-transformed counterparts (Figure 1A). ROS scavenger vitamin E diminished, whereas MTH1 inhibitor SCH51344 (MTH1 sanitizes oxidized dNTP pools to prevent incorporation of damaged bases during DNA replication [36]) enhanced the toxic effect of olaparib in JAK2(V617F)+EpoR, MPL(W515L) and CALR(del52)+MPL(wt) cells.

Most of key proteins regulating major DSB repair pathways, HR, D-NHEJ and B-NHEJ were either not affected or upregulated in the presence of JAK2(V617F), MPL(W515L) and CALR(del52) (Figure 1B). However, it appears that expression of MPL(W515L) caused approximately 2-fold reduction of the expression of BRCA1 and BRCA2 proteins. Since activation of MPL is associated with upregulation of D-NHEJ [37], it is plausible that BRCA1/2-mediated HR plays a secondary role in DSB repair in MPL(W515L)-positive cells as reflected by downregulated BRCA proteins.

Next, the sensitivity to PARP inhibitors of primary Lin^-CD34^+ cells from healthy donors and MPN patients expressing JAK2(V617F), MPL(W515L), and CALR(del52) were tested in a clonogenic assay (Figure 2). Lin^-CD34^+ cells isolated from healthy donors were only partially sensitive to olaparib and BMN673 (Figure 2A). Eight JAK2(V617F) samples (6109-K, 013-S, 034-S, 8729-K, 338-S, 742-K, 4082-K, 1-P) were sensitive, whereas 3 samples (288-S, 4552-K, 10141-K) were only partially sensitive to olaparib and BMN673 (Figure 2B). On the other hand, CALR(del52) samples displayed highest variability in sensitivity to PARP inhibitors, from sensitive (168-S and CV096-G), partially sensitive (055-S, 073-S, 215-S), to resistant (109-S) (Figure 2C). MPL(ex10mut) samples behaved similar to JAK2(V617F) samples by being sensitive (PF4594-G, BT74-G, MB76-G, BA7621-G) or partially sensitive (RB3382-G) to PARP inhibitors (Figure 2D).

Ruxolitinib inhibited DSB repair and enhanced the sensitivity of MPN cells to PARP inhibitors

BaF3-JAK2(V617F)+EpoR, 32Dcl3-MPL(W515L), and 32Dcl3-CALR(del52)+MPL(wt) cells treated with olaparib and/or ruxolitinib accumulated elevated numbers of DSBs, especially in cells treated with ruxolitinib and olaparib (Figure 3A, upper panel). In addition, enhanced accumulation of DSBs in ruxolitinib + olaparib –treated JAK2(V617F)+EpoR, MPL(W515L) and CALR(del52)+MPL(wt) –positive cells was associated with synergistic increase of cell death (Figure 3A, lower panel).

To determine if ruxolitinib-mediated accumulation of olaparib-induced DSBs is associated with inhibition of DSB repair activity we performed a Western blot array to assess expression of key proteins in DSB repair pathways. JAK2(V617F)+EpoR, MPL(W515L), and CALR(del52)+MPL(wt) –positive cells and their parental counterparts were treated with ruxolitinib for 24 hrs in the presence of IL3 + Epo to inhibit JAK2 kinases as documented by downregulated phospho-STAT5A(Ser780) (Figure 3B). At the same time, ruxolitinib-treated cells were viable as assessed by Trypan blue exclusion, minimal caspase-3 activation, and uncleaved PARP1. Key proteins in HRR (BRCA1 and RAD51) and D-NHEJ (Lig4), but not B-NHEJ were downregulated in ruxolitinib-treated JAK2(V617F)+EpoR, MPL(W515L), and CALR(del52)+MPL(wt) –positive cells (Figure 3B).

Next, we examined if ruxolitinib-induced downregulation of RAD51 and LIG4 proteins (Figure 3C, upper panel) caused reduction of HRR and D-NHEJ activities. D-NHEJ activity measured in vitro by nuclear cell lysate –mediated plasmid end-joining was inhibited by approximately 3-fold in ruxolitinib-treated JAK2(V617F)-positive cells (Figure 3C, middle panel). To measure HRR activity an I-SceI endonuclease-mediated DSB was induced in Jak2(V617F)-positive Ba/F3-HR2 cells carrying HR-EGFP recombination reporter cassette integrated in their genome. HRR restores the expression of GFP detected by flow cytometry. Ruxolitinib-treated

Ba/F3-HR2 cells displayed approximately 2-fold reduction in HRR activity (Figure 3C, lower panel).

We have previously reported that D-NHEJ-deficient quiescent and HRR/D-NHEJ-deficient proliferating tumor cells were sensitive to dual cellular synthetic lethality exerted by PARPi [33]. Therefore, we tested if ruxolitinib-induced downregulation of D-NHEJ and HRR sensitize JAK2(V617F)-positive quiescent and proliferating cells, respectively, to PARPi-mediated synthetic lethality. Intriguingly, ruxolitinib enhanced the sensitivity of LSCs-enriched $Lin^-CD34^+CD38^-CTV^{low}$ proliferating patient cells to olaparib (Figure 3D,E). Moreover, even if individual drugs did not affect LSCs-enriched $Lin^-CD34^+CD38^-CTV^{max}$ quiescent cells, the combination exerted synergistic inhibitory effect (Figure 3D,E).

Ruxolitinib enhanced the effect of PARP inhibitors and/or hydroxyurea in vitro in pre-selected MNP samples

Clonogenic assay revealed that Lin^-CD34^+ primary MPN cells from a cohort of MPNs expressing JAK2(V617F), MPL(ex10mut), and CALR(del52), which were sensitive to PARPi (Figure 2B-D, optimal response), responded favorably to the combination of ruxolitinib + olaparib and ruxolitinib + hydroxyurea + olaparib (034-S, 338-S, 742-K, 013-S, 4082-K, 6109-K, 8729-K, 168-S, CV096-K, PF4594-G, BT74-G, MB76-G, BA7621-G in Figure 4A-C, D-left panel). On the other hand, cells from samples displaying partial sensitivity or resistance to PARPi (suboptimal response) could be sub-divided in to two cohorts: these which responded favorably (055-S, 215-S in Figure 4A-C, D-middle left panel) or unfavorably (10141-K, 5442-K, 288-S, 073-S, 109-S, RB3382-G in Figure 4A-C, D- middle right panel) to ruxolitinib + olaparib and/or ruxolitinib + hydroxyurea + olaparib. Lin^-CD34^+ cells from 3 healthy donors displayed homogenous response pattern to the drugs (Figure 4D- right panel), similar to that of unfavorable MPN cohort (Figure 4D- middle right panel).

Ruxolitinib enhanced the effect of PARP inhibitors and/or hydroxyurea in a retroviral murine model of JAK2(V617F)-positive MPN

To test if ruxolitinib enhances the effect of PARPi +/- standard cytotoxic drug hydroxyurea, we applied a murine model of GFP+JAK2(V617F)-positive PV (Figure 5A) [3]. BMN673 was used here because it displays better pharmacokinetic parameters in mice than olaparib [38]. As expected, ruxolitinib and hydroxyurea when used individually did not reduce the percentage of GFP+JAK2(V617F)-positive cells in peripheral blood, spleen and bone marrow, and BMN673 exerted only a very moderate inhibitory effect (Figure 5B-D). However, ruxolitinib significantly enhanced the therapeutic effect of BMN673 and of BMN673 plus hydroxyurea. In addition, the population of stem cell-enriched GFP+$Lin^{-}Sca\text{-}1^{+}c\text{-}Kit^{+}$ JAK2(V617F) cells was significantly reduced in mice treated with ruxolitinib combined with BMN673 or BMN673 + hydroxyurea when compared to BMN673 +/- hydroxyurea (Figure 5E).

Major organs such as heart, lungs, liver, kidneys, bone marrow and spleen in mice treated with combination of ruxolitinib, hydroxyurea and BMN67 showed normal morphologic features with no evidence of ischemia or drug toxicity (Supplementary Figure S1). More detailed analysis of hematopoietic system revealed only transient moderate toxicity in peripheral blood and bone marrow (Supplementary Table 2).

In vivo PARP inhibitor treatment enhanced the effect of ruxolitinib + hydroxyurea against pre-selected primary MPN xenografts in immunodeficient mice

Primary MPN samples [JAK2(V617F) –positive 6109-K, MPL(ex10mut)-positive PF4594-G, and CALR(del52)-positive 168-S] were pre-selected based on their favorable response to PARPi +/- ruxolitinib and hydroxyurea (Figure 2B-D and 4A-C). Primary $Lin^{-}CD34^{+}$ MPN cells from these patients also engrafted in NRGS mice (>5% hCD45+ cells in peripheral blood and splenomegaly after 3 weeks). NRSG mice bearing these MPN xenografts were treated with vehicle (Control), hydroxyurea + ruxolitinib (HR), BMN673, or HR + BMN673 (Figure 6A). The therapeutic effect

was measured by detection of $hCD45^+$ cells in peripheral blood, spleen and bone marrow, and of $hCD45^+Lin^-CD34^+$ and $hCD45^+Lin^-CD34^+CD38^-$ cells in bone marrow.

Ruxolitinib + hydroxyurea did not consistently reduce the percentage and number of MPN xenograft cells (Figure 6B). On the other hand BMN673 reduced the percentage of $hCD45^+$ cells in peripheral blood, spleen and bone marrow, and the number of $hCD45^+Lin^-CD34^+$ and $hCD45^+Lin^-CD34^+CD38^-$ cells in bone marrow of mice bearing JAK2(V617F), MPL(ex10mut), and CALR(del52)-positive MPN xenografts. Importantly, the combination of BMN673 + ruxolitinib + hydroxyurea exerted the strongest anti-MPN effect when compared to BMN673 and ruxolitinib + hydroxyurea.

Discussion

Our data and other reports indicated that MPN cells contain elevated levels of ROS and stalled replication forks, resulting in accumulation of potentially lethal DSBs [8,12]. However, MPN cells are able to repair numerous DSBs because two major DSB repair pathways, HRR and D-NHEJ, are activated [31,37]. PARPi and/or hydroxyurea generate additional DSBs which may overwhelm DSB repair activity in some MPN cells to cause cell death [39,40], but numerous cells can survive the treatment.

We have shown here that JAK1/2 kinase inhibitor ruxolitinib caused downregulation of key members of HRR (BRCA1, RAD51) and D-NHEJ (LIG4) in JAK2(V617F), MPL(ex10mut), and CALR(del52)-positive cell lines resulting in reduced HRR and D-NHEJ activities. This effect was associated with PARPi-induced accumulation of DSBs and enhanced elimination of MPN cells from numerous patient samples. Since defects in DNA repair sensitized tumor cells to PARPi, we postulate that ruxolitinib-induced HRR and D-NHEJ -deficiencies triggered PARPi-mediated synthetic lethality [41].

All three “driver” mutations, [JAK2(V617F), CALR(del52), and MPL(W515L)] have been detected not only in mature MPN cells, but also in MPN stem cells, and therefore these cells

must be eliminated to eradicate the disease [42-45]. Since JAK1/2i did not eliminate the disease-initiating population novel therapeutic approaches were needed [4].

Ruxolitinib treatment inhibits proliferation of JAK2(V617), CALR(del52) and MPL(W515L)-positive cells, but induce minimal degrees of apoptosis ([46] and Supplementary Figure S2), and growth-arrested cells usually show poor sensitivity to cytotoxic drugs. We observed that ruxolitinib reduced the activity of DSB repair pathways playing a key role in proliferating (HRR/D-NHEJ) and quiescent (D-NHEJ) cells. We postulate that ruxolitinib-mediated inhibition of HR and D-NHEJ creates a unique opportunity to trigger PARPi-mediated dual synthetic lethality in HRR and D-NHEJ –deficient proliferating cells and in D-NHEJ –deficient G1/G0 cells expressing the "driver" mutations.

This statement is supported by 5 observations: (1) quiescent and proliferating $Lin^-CD34^+CD38^-$ human MPN-initiating cells [42] were eliminated in vitro by ruxolitinib + olaparib, (2) $Lin^-Sca\text{-}1^+c\text{-}Kit^+$ murine MPN initiating cells [4,43] were eliminated by ruxolitinib + BMN673 +/- hydroxyurea in syngeneic mice bearing JAK2(V617F)-positive MPN-like disease, (3) $Lin^-CD34^+CD38^-$ human MPN-initiating cells were eliminated by ruxolitinib + BMN673 +/- hydroxyurea in NRGS mice bearing primary MPN xenografts, (4) disease-initiating cells capable to engraft secondary recipient mice were eliminated by ruxolitinib + BM3673 + hydroxyurea in NRGS mice bearing primary MPN xenograft (Supplementary Figure S3), and (5) we reported that PARPi eliminated HRR/D-NHEJ deficient proliferating and D-NHEJ deficient quiescent acute and chronic leukemia cells [33]. It has been reported that interferon alpha, which to date shows the highest degree of molecular remissions among the conventional drugs used to treat MPN patients, induced proliferation of JAK2(V617F) disease-initiating cells and promoted a predetermined erythroid differentiation [47]. Our approach directly eliminates both proliferating and quiescent MPN-initiating cells, thus significantly expanding the MPN cells that can be targeted to the most primitive cell population.

Individual MPN samples displayed high level of variability in responding to PARPi. Another report supported this observation and suggested that sensitivity to PARPi was associated with impaired HRR [48]. Ruxolitinib induced HRR and D-NHEJ deficiency and enhanced sensitivity to PARPi in numerous patient samples which displayed optimal and sub-optimal response to PARPi used alone. However, a cohort of MPN samples with sub-optimal response to PARPi remained partially resistant to the inhibitor even when combined with ruxolitinib. There are several possible explanations for the heterogeneous response of individual MPNs to PARPi or ruxolitinib + PARPi.

First, additional genetic/epigenetic factors inherently characteristic for individual MPNs [e.g., mutations in TET2, ASXL1, DNMT3A, EZH2, IDH1 [2]] may regulate sensitivity to PARPi +/- ruxolitinib. This is supported by the data suggesting that TET2 affects the response of JAK2(V617F)-positive murine bone marrow cells to olaparib +/- ruxolitinib (Supplementary Figure S4), that mutations in DNMT3a and IDH1 altered DNA repair activity and sensitivity to PARPi and anthracycyline [49-51], and that EZH2 downregulates the expression of BRCA1 and RAD51 [52-55]. In addition, deletion of *Asxl1* and/or *Tet2* deregulated expression of DNA repair genes including *Rad51* in $Lin^{-}Sca\text{-}1^{+}c\text{-}Kit^{+}$ murine bone marrow cells [56]. The hypothesis that accompanying mutations may modulate sensitivity of MPN cells to PARPi +/- JAK1/2i is further supported by our data from primary cells indicating that TET2mut, EZH2mut and ASXL1mut may enhance while DNMT3Amut alone and RUNX1mut may diminish sensitivity to PARPi used as single agents and also combined with ruxolitinib +/- hydroxyurea (Supplementary Figure S5). In addition, mutations in the BRCA1-BRCA2-containing complex 3 (BRCC3) gene implicated in DNA repair are frequently concomitant with JAK2 and MPL mutations and may modulate the sensitivity to PARPi [57].

Although heterozygosity/homozygosity of the mutated “driver” allele does not appear to regulate sensitivity to olaparib (Supplementary Figure S6A), it may affect the response to the combination of ruxolitinib + hydroxyurea + olaparib (Supplementary Figure S6B). The mutant

allele burden did not appear to influence PARPi efficacy (Supplementary Figure S7, Figure 2 and Supplementary Table 1).

In conclusion, we demonstrated that JAK1/2i-induced DNA repair deficiencies may be clinically explored in pre-selected MPN patients treated with a combination of ruxolitinib and, as innovative therapeutic approach, PARPi +/- hydroxyurea to enhance elimination of MPN-initiating and progenitor cell populations. All of these drugs have been approved as therapeutic agents in oncology thus facilitating such a clinical trial. Moreover, similar therapeutic approach could be undertaken also in other hematological malignancies displaying constitutive activation of JAK kinases either by direct mutation [e.g., JAK2(R683S) in pediatric acute lymphoblastic leukemia [58] and JAK3(A572V) in acute megakaryocytic leukemia [59]] or by activating mutation upstream of JAK kinases [e.g., CSF3R(T618I) in chronic neutrophilic leukemia [60]], because cells lines transformed with these mutants were sensitive to the combination of ruxolitinib and olaparib (Supplementary Figure S8).

Acknowledgements

This work was supported by the Leukemia and Lymphoma Society Quest-for-Cure grant 0860-15 and NIH/NCI CA134458 (T. Skorski). S.F. was supported by the grant from NCN No. 2013/11/B/NZ7/02248 and B.V.L. was supported by the European Union's Horizon 2020 research and innovation program under Marie Sklodowska-Curie grant agreement no. 665735 and by funding from Polish Ministry of Science and Higher Education for the implementation of international projects. Work in the T.G. lab was supported by the Cambridge NIHR Biomedical Research Center and by the Wellcome Trust-Medical Research Council Cambridge Stem Cell Institute. We would like to thank Dr. Ann Mullally (Division of Hematology, Department of Medicine, Brigham and Women's Hospital, Harvard Medical School, Boston, MA, USA) for providing murine *Tet2-/-*, *Tet2+/+*, *Jak2(V617F);Tet2-/-* and *Jak2(V617F);Tet2+/+* cells, Dr. Charkes Mullighan (St. Jude Children's research Hospital, Memphis, TN, USA) for providing

BaF3-EpoR cells expressing JAK2(R683S), Dr. Jeffrey Taub (Children's Hospital of Michigan, Detroit, MI, USA) for providing CMK cells carrying JAK3(A572V), and Dr. Jeffrey Tyner (Oregon Health and Science University, Portland, OR, USA) for providing BaF3 cells expressing CSF3R(T618I).

Authorship: M.N-S. performed in vitro studies with patient samples and run Western analyses. S.M. tested DNA repair activity and analyzed mice bearing primary MPN xenografts. Y.D. analyzed mice bearing MPNs. K.S. analyzed mice bearing MPNs. S.F. determined sample sensitivity in the context of allele burden. B.V.L. analyzed heterozygous/homozygous cells. M.S. performed experiments with cell lines. E.A.B. performed histopathology analyses. L.K. provided murine cells for in vivo studies. M.N. examined sensitivity of cells expressing MPN-unrelated mutants. M.K. performed NGS analysis of MPN samples. H.Z. performed statistical analyses. J.P., S.K., T.G. provided MPN primary cells. R.S. provided MPN primary cells and murine cells. M.W. supervised E.A.B. K.P. supervised B.V.L. T.S. conceived the idea, supervised the project and wrote the final version of the manuscript. All authors read, corrected and approved the final version of the manuscript.

Conflict-of-interest disclosure: S.K. reports having received honoraria and travel support for conferences by Novartis, Incyte, and Bristol-Myers Squibb. All other authors declare no conflict of interest.

References

1. Lundberg P, Karow A, Nienhold R, et al. Clonal evolution and clinical correlates of somatic mutations in myeloproliferative neoplasms. *Blood*. 2014;123(14):2220-2228.
2. Delic S, Rose D, Kern W, et al. Application of an NGS-based 28-gene panel in myeloproliferative neoplasms reveals distinct mutation patterns in essential thrombocythaemia, primary myelofibrosis and polycythaemia vera. *Br J Haematol*. 2016.
3. Kubovcakova L, Lundberg P, Grisouard J, et al. Differential effects of hydroxyurea and INC424 on mutant allele burden and myeloproliferative phenotype in a JAK2-V617F polycythemia vera mouse model. *Blood*. 2013;121(7):1188-1199.

4. Mullally A, Lane SW, Ball B, et al. Physiological Jak2V617F expression causes a lethal myeloproliferative neoplasm with differential effects on hematopoietic stem and progenitor cells. *Cancer Cell*. 2010;17(6):584-596.
5. Campbell PJ, Green AR. The myeloproliferative disorders. *N Engl J Med*. 2006;355(23):2452-2466.
6. Barosi G, Vannucchi AM, De Stefano V, et al. Identifying and addressing unmet clinical needs in Ph-neg classical myeloproliferative neoplasms: a consensus-based SIE, SIES, GITMO position paper. *Leuk Res*. 2014;38(2):155-160.
7. Mascarenhas MI, Bacon WA, Kapeni C, et al. Analysis of Jak2 signaling reveals resistance of mouse embryonic hematopoietic stem cells to myeloproliferative disease mutation. *Blood*. 2016;127(19):2298-2309.
8. Marty C, Lacout C, Droin N, et al. A role for reactive oxygen species in JAK2 V617F myeloproliferative neoplasm progression. *Leukemia*. 2013;27(11):2187-2195.
9. Sattler M, Winkler T, Verma S, et al. Hematopoietic growth factors signal through the formation of reactive oxygen species. *Blood*. 1999;93(9):2928-2935.
10. Yoshida K, Kirito K, Yongzhen H, Ozawa K, Kaushansky K, Komatsu N. Thrombopoietin (TPO) regulates HIF-1alpha levels through generation of mitochondrial reactive oxygen species. *Int J Hematol*. 2008;88(1):43-51.
11. Jia L, Xu M, Zhen W, et al. Novel anti-oxidative role of calreticulin in protecting A549 human type II alveolar epithelial cells against hypoxic injury. *Am J Physiol Cell Physiol*. 2008;294(1):C47-55.
12. Chen E, Ahn JS, Massie CE, et al. JAK2V617F promotes replication fork stalling with disease-restricted impairment of the intra-S checkpoint response. *Proc Natl Acad Sci U S A*. 2014;111(42):15190-15195.
13. Viale A, De Franco F, Orleth A, et al. Cell-cycle restriction limits DNA damage and maintains self-renewal of leukaemia stem cells. *Nature*. 2009;457(7225):51-56.
14. Horibe S, Takagi M, Unno J, et al. DNA damage check points prevent leukemic transformation in myelodysplastic syndrome. *Leukemia*. 2007;21(10):2195-2198.
15. Cavelier C, Didier C, Prade N, et al. Constitutive activation of the DNA damage signaling pathway in acute myeloid leukemia with complex karyotype: potential importance for checkpoint targeting therapy. *Cancer Res*. 2009;69(22):8652-8661.
16. Boehrer S, Ades L, Tajeddine N, et al. Suppression of the DNA damage response in acute myeloid leukemia versus myelodysplastic syndrome. *Oncogene*. 2009;28(22):2205-2218.
17. Sallmyr A, Fan J, Rassool FV. Genomic instability in myeloid malignancies: increased reactive oxygen species (ROS), DNA double strand breaks (DSBs) and error-prone repair. *Cancer Lett*. 2008;270(1):1-9.
18. Callen E, Jankovic M, Difilippantonio S, et al. ATM prevents the persistence and propagation of chromosome breaks in lymphocytes. *Cell*. 2007;130(1):63-75.
19. Hasham MG, Donghia NM, Coffey E, et al. Widespread genomic breaks generated by activation-induced cytidine deaminase are prevented by homologous recombination. *Nat Immunol*. 2010;11(9):820-826.
20. Krejci O, Wunderlich M, Geiger H, et al. p53 signaling in response to increased DNA damage sensitizes AML1-ETO cells to stress-induced death. *Blood*. 2008;111(4):2190-2199.
21. Hoser G, Majsterek I, Romana DL, Slupianek A, Blasiak J, Skorski T. Fusion oncogenic tyrosine kinases alter DNA damage and repair after genotoxic treatment: role in drug resistance? *Leuk Res*. 2003;27(3):267-273.
22. Chapman JR, Taylor MR, Boulton SJ. Playing the end game: DNA double-strand break repair pathway choice. *Mol Cell*. 2012;47(4):497-510.

23. Karanam K, Kafri R, Loewer A, Lahav G. Quantitative live cell imaging reveals a gradual shift between DNA repair mechanisms and a maximal use of HR in mid S phase. *Mol Cell*. 2012;47(2):320-329.
24. Feng Z, Scott SP, Bussen W, et al. Rad52 inactivation is synthetically lethal with BRCA2 deficiency. *Proc Natl Acad Sci U S A*. 2011;108(2):686-691.
25. Bryant HE, Petermann E, Schultz N, et al. PARP is activated at stalled forks to mediate Mre11-dependent replication restart and recombination. *EMBO J*. 2009;28(17):2601-2615.
26. Ying S, Chen Z, Medhurst AL, et al. DNA-PKcs and PARP1 Bind to Unresected Stalled DNA Replication Forks Where They Recruit XRCC1 to Mediate Repair. *Cancer Res*. 2016;76(5):1078-1088.
27. Cramer-Morales K, Nieborowska-Skorska M, Scheibner K, et al. Personalized synthetic lethality induced by targeting RAD52 in leukemias identified by gene mutation and expression profile. *Blood*. 2013;122(7):1293-1304.
28. Han L, Schubert C, Kohler J, et al. Calreticulin-mutant proteins induce megakaryocytic signaling to transform hematopoietic cells and undergo accelerated degradation and Golgi-mediated secretion. *J Hematol Oncol*. 2016;9(1):45.
29. Pikman Y, Lee BH, Mercher T, et al. MPLW515L is a novel somatic activating mutation in myelofibrosis with myeloid metaplasia. *PLoS Med*. 2006;3(7):e270.
30. Walz C, Crowley BJ, Hudon HE, et al. Activated Jak2 with the V617F point mutation promotes G1/S phase transition. *J Biol Chem*. 2006;281(26):18177-18183.
31. Plo I, Nakatake M, Malivert L, et al. JAK2 stimulates homologous recombination and genetic instability: potential implication in the heterogeneity of myeloproliferative disorders. *Blood*. 2008;112(4):1402-1412.
32. Slupianek A, Nowicki MO, Koptyra M, Skorski T. BCR/ABL modifies the kinetics and fidelity of DNA double-strand breaks repair in hematopoietic cells. *DNA Repair (Amst)*. 2006;5(2):243-250. Epub 2005 Nov 2016.
33. Nieborowska-Skorska M, Sullivan K, Dasgupta Y, et al. Gene expression and mutation-guided synthetic lethality eradicates proliferating and quiescent leukemia cells. *J Clin Invest*. 2017;127(6):2392-2406.
34. Goyama S, Wunderlich M, Mulloy JC. Xenograft models for normal and malignant stem cells. *Blood*. 2015;125(17):2630-2640.
35. Slinker BK. The statistics of synergism. *J Mol Cell Cardiol*. 1998;30(4):723-731.
36. Gad H, Koolmeister T, Jemth AS, et al. MTH1 inhibition eradicates cancer by preventing sanitation of the dNTP pool. *Nature*. 2014;508(7495):215-221.
37. de Laval B, Pawlikowska P, Petit-Cocault L, et al. Thrombopoietin-increased DNA-PK-dependent DNA repair limits hematopoietic stem and progenitor cell mutagenesis in response to DNA damage. *Cell Stem Cell*. 2013;12(1):37-48.
38. Shen Y, Rehman FL, Feng Y, et al. BMN 673, a novel and highly potent PARP1/2 inhibitor for the treatment of human cancers with DNA repair deficiency. *Clin Cancer Res*. 2013;19(18):5003-5015.
39. Petermann E, Orta ML, Issaeva N, Schultz N, Helleday T. Hydroxyurea-stalled replication forks become progressively inactivated and require two different RAD51-mediated pathways for restart and repair. *Mol Cell*. 2010;37(4):492-502.
40. Yang KS, Kohler RH, Landon M, Giedt R, Weissleder R. Single cell resolution in vivo imaging of DNA damage following PARP inhibition. *Sci Rep*. 2015;510129.
41. Dietlein F, Thelen L, Reinhardt HC. Cancer-specific defects in DNA repair pathways as targets for personalized therapeutic approaches. *Trends Genet*. 2014;30(8):326-339.
42. Jamieson CH, Gotlib J, Durocher JA, et al. The JAK2 V617F mutation occurs in hematopoietic stem cells in polycythemia vera and predisposes toward erythroid differentiation. *Proc Natl Acad Sci U S A*. 2006;103(16):6224-6229.

43. Lundberg P, Takizawa H, Kubovcakova L, et al. Myeloproliferative neoplasms can be initiated from a single hematopoietic stem cell expressing JAK2-V617F. *J Exp Med*. 2014;211(11):2213-2230.
44. Nangalia J, Massie CE, Baxter EJ, et al. Somatic CALR mutations in myeloproliferative neoplasms with nonmutated JAK2. *N Engl J Med*. 2013;369(25):2391-2405.
45. Chaligne R, James C, Tonetti C, et al. Evidence for MPL W515L/K mutations in hematopoietic stem cells in primitive myelofibrosis. *Blood*. 2007;110(10):3735-3743.
46. Mazzacurati L, Lambert QT, Pradhan A, Griner LN, Huszar D, Reuther GW. The PIM inhibitor AZD1208 synergizes with ruxolitinib to induce apoptosis of ruxolitinib sensitive and resistant JAK2-V617F-driven cells and inhibit colony formation of primary MPN cells. *Oncotarget*. 2015;6(37):40141-40157.
47. Mullally A, Bruedigam C, Poveromo L, et al. Depletion of Jak2V617F myeloproliferative neoplasm-propagating stem cells by interferon-alpha in a murine model of polycythemia vera. *Blood*. 2013;121(18):3692-3702.
48. Pratz KW, Koh BD, Patel AG, et al. Poly (ADP-Ribose) Polymerase Inhibitor Hypersensitivity in Aggressive Myeloproliferative Neoplasms. *Clin Cancer Res*. 2016;22(15):3894-3902.
49. Sulkowski PL, Corso CD, Robinson ND, et al. 2-Hydroxyglutarate produced by neomorphic IDH mutations suppresses homologous recombination and induces PARP inhibitor sensitivity. *Sci Transl Med*. 2017;9(375).
50. Guryanova OA, Shank K, Spitzer B, et al. DNMT3A mutations promote anthracycline resistance in acute myeloid leukemia via impaired nucleosome remodeling. *Nat Med*. 2016;22(12):1488-1495.
51. Inoue S, Li WY, Tseng A, et al. Mutant IDH1 Downregulates ATM and Alters DNA Repair and Sensitivity to DNA Damage Independent of TET2. *Cancer Cell*. 2016;30(2):337-348.
52. Gonzalez ME, DuPrie ML, Krueger H, et al. Histone methyltransferase EZH2 induces Akt-dependent genomic instability and BRCA1 inhibition in breast cancer. *Cancer Res*. 2011;71(6):2360-2370.
53. Zeidler M, Varambally S, Cao Q, et al. The Polycomb group protein EZH2 impairs DNA repair in breast epithelial cells. *Neoplasia*. 2005;7(11):1011-1019.
54. Li T, Cai J, Ding H, Xu L, Yang Q, Wang Z. EZH2 participates in malignant biological behavior of epithelial ovarian cancer through regulating the expression of BRCA1. *Cancer Biol Ther*. 2014;15(3):271-278.
55. Yang Q, Nair S, Laknaur A, Ismail N, Diamond MP, Al-Hendy A. The Polycomb Group Protein EZH2 Impairs DNA Damage Repair Gene Expression in Human Uterine Fibroids. *Biol Reprod*. 2016;94(3):69.
56. Abdel-Wahab O, Gao J, Adli M, et al. Deletion of Asxl1 results in myelodysplasia and severe developmental defects in vivo. *J Exp Med*. 2013;210(12):2641-2659.
57. Huang D, Nagata Y, Grossmann V, et al. BRCC3 mutations in myeloid neoplasms. *Haematologica*. 2015;100(8):1051-1057.
58. Mullighan CG, Zhang J, Harvey RC, et al. JAK mutations in high-risk childhood acute lymphoblastic leukemia. *Proc Natl Acad Sci U S A*. 2009;106(23):9414-9418.
59. Xavier AC, Edwards H, Dombkowski AA, et al. A unique role of GATA1s in Down syndrome acute megakaryocytic leukemia biology and therapy. *PLoS One*. 2011;6(11):e27486.
60. Maxson JE, Gotlib J, Pollyea DA, et al. Oncogenic CSF3R mutations in chronic neutrophilic leukemia and atypical CML. *N Engl J Med*. 2013;368(19):1781-1790.

Figure legends:

Figure 1. Sensitivity of JAK2(V617F), CALR(del52), and MPL(ex10mut) -positive cells to PARP inhibitors. (**A**) Cell lines expressing JAK2(V617F)+EpoR, CALR(del52) + MPL(wt), or MPL(W515L) were incubated with olaparib alone (1.25, 2.5, 5.0 μM) (squares) or BMN673 alone (12.5, 25.0, 50.0 nM) (squares), olaparib + 200 μM vitamin E (circles), or olaparib + 2.5 μM SCH51344 (triangles) for 96 hrs in the presence of IL-3 + Epo. Parental cells (diamonds) were incubated with olaparib or BMN673 only. Living cells were counted in Trypan blue. Results represent mean ± SD percent of living cells in comparison to untreated control from 3 independent experiments. (**B**) Western analysis of the indicated proteins in parental cells (P) and in isogenic cells expressing JAK2(V617F)+EpoR, CALR(del52)+MPL(wt) and MPL(W515L).

Figure 2. Sensitivity of individual MPN samples expressing JAK2(V617F), CALR(del52), and MPL(ex10mut) to PARP inhibitors. Lin^-CD34^+ primary cells from (**A**) healthy donors (n=3) and from (**B**) JAK2(V617F), (**C**) CALR(del52), (**D**) MPL(ex10mut) –positive MPN patients were incubated with olaparib (1.25, 2.5, 5.0 μM) or BMN673 (12.5, 25.0, 50.0 nM) for 96 hrs in the presence of growth factors [100 ng/ml SCF; 10 ng/ml Flt3 ligand; 20 ng/ml IL-3, IL-6, G-CSF and GM-CSF; 12 units/ml EPO; 2.5 ng/ml TPO] followed by plating in methylcellulose. Colonies were counted after 7-10 days. Results represent % of colonies in comparison to untreated control.

Figure 3. JAK2 kinase inhibitor ruxolitinib reduced HRR and D-NHEJ activity and enhanced the anti-MPN effect of PARP inhibitor olaparib. (**A**) Parental cell lines and these expressing JAK2(V617F)+EpoR, CALR(del52) + MPL(wt), or MPL(W515L) were untreated (C)

or treated with 5μM olaparib (O) or 400 nM ruxolitinib (R) or ruxolitinib + olaparib (R+O) in the presence of IL-3 + Epo for 24 hrs (γ-H2AX) and 96 hrs (cell survival). DSBs were detected by γ-H2AX immunofluorescence overlapping with DAPI (upper panel), and living cells were counted in Trypan blue (lower panel; percent of living cells in comparison to untreated control). Results represent means ± SD from 3 independent experiments. *p<0.05 in comparison to C using Student t test; **p≤0.001 in comparison to R and O groups using the response additivity approach. (**B**) Western analysis of the indicated proteins in cells expressing JAK2(V617F)+EpoR, CALR(del52)+MPL and MPL(W515L), and in BaF3-EpoR cells (Parental) after 24 hrs incubation with 400 nM ruxolitinib in the presence of IL-3 + Epo. Proteins downregulated by ruxolitinib are in red boxes. (**C**) HRR and D-NHEJ activities in JAK2(V617F)-positive cells untreated (-) or treated for 24 hrs with 400 nM ruxolitinib (+). Upper panel: Western blots, Middle panel: D-NHEJ activity, S – linearized plasmid substrate, P – ligated plasmid products, results show % of P; Lower panel: HRR activity measured by restoration of EGFP expression, results show % of GFP+ cells; *p≤0.01. (**D**) Number of proliferating $Lin^-CD34^+CD38^-CTV^{low}$ and quiescent $Lin^-CD34^+CD38^-CTV^{max}$ cells from individual JAK2(V617F)-positive MPN samples left untreated (C) or treated with ruxolitinib (R, 25 nM), olaparib (O, 1.25 μM) and ruxolitinib + olaparib (R+O). (**E**) Cumulative percentages from samples examined in panel **D**; *p<0.001 in comparison to R or O groups using Student t test; **p<0.01 in comparison to R and O groups using the response additivity approach.

Figure 4. The effect of ruxolitinib on the sensitivity of JAK2(V617F), CALR(del52), and MPL(ex10mut) MPN cells to PARP inhibitors. Lin^-CD34^+ cells from PV, ET and MF patients carrying (**A**) JAK2(V617F), (**B**) CALR(del52), and (**C**) MPL(ex10mut) were incubated with olaparib (O, 1.25 μM), hydroxyurea (H, 10 μM) and/or ruxolitinib (R, 25 nM) for 72 hrs in the presence of growth factors (see Figure 2) and plated in methylcellulose. Colonies were counted

after 7-10 days. Results represent mean number of colonies ± SD from triplicates. (**D**) Ruxolitinib (R)-treated Lin^-CD34^+ cells from cohorts of MPN samples (black bars) and healthy donors (grey bars) displayed heterogenic sensitivity to PARP inhibitor; *p<0.05 in comparison to O and **p<0.05 in comparison to HO using Student t test.

Figure 5. BMN673 exerted anti-MPN effect in vivo. (**A**) Experimental model. Lethally irradiated C57BL/6 recipient mice were injected with 1:1 mixture of 10^6 GFP+JAK2(V671F) and 10^6 wild-type bone marrow cells. Five weeks later mice were treated with vehicle (C), hydroxyurea (H; 30 mg/kg BID i.p.), ruxolitinib (R; 30 mg/kg BID oral gavage), BMN673 (B; 0.33 mg/kg i.v.), H+R, H+B, R+B, and H+R+B for 3 weeks. Percent of GFP+JAK2(V617F) was measured in (**B**) bone marrow cells, (**C**) splenocytes, and (**D**) peripheral blood leukocytes; (**E**) number of GFP+JAK2(V617F) $Lin^-Sca1^+c\text{-}Kit^+$ (LSK) cells per 10^6 bone marrow cells was calculated, too. *, **, and *** - p<0.05 when compared to control, single treatment and double treatment, respectively, from 6-7 mice using Student t test.

Figure 6. BMN673 exerted anti-MPN xenograft effect in vivo. (**A**) Experimental model. Sub-lethally irradiated NRGS recipient mice were injected with 10^6 primary Lin^- MPN cells from individual MPN patients expressing JAK2(V617F), CALR(del52), or MPL(W515L). One week later mice were treated with vehicle (C), hydroxyurea (H; 30 mg/kg BID i.p.) + ruxolitinib (R; 30 mg/kg BID oral gavage) (HR), BMN673 (B; 0.33 mg/kg i.v.) and HR+B (HRB) for 3 weeks (3-5 mice/group). Indicated cells were detected by immunofluorescence. (**B**) Percent of hCD45+ cells was measured in peripheral blood leukocytes (PBLs), splenocytes (SPLs) and bone marrow cells (BMCs). Number of $hCD45^+$ BMCs expressing Lin^-CD34^+ and $Lin^-CD34^+CD38^-$ per

10^6 cells were determined. * and ** - $p<0.05$ in comparison to C and all other groups, respectively, using Student t test.

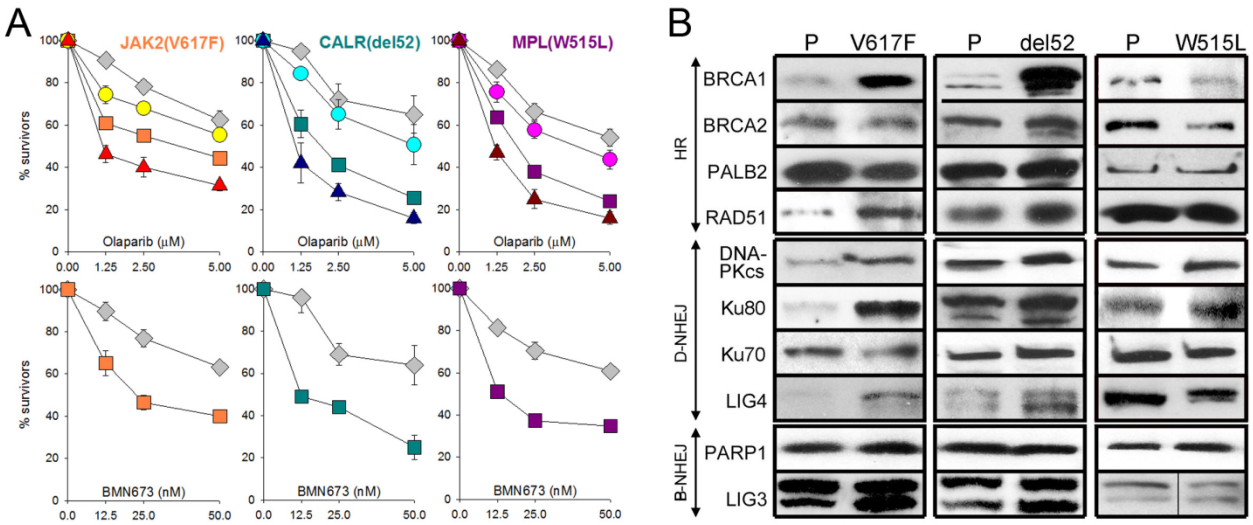

Figure 1

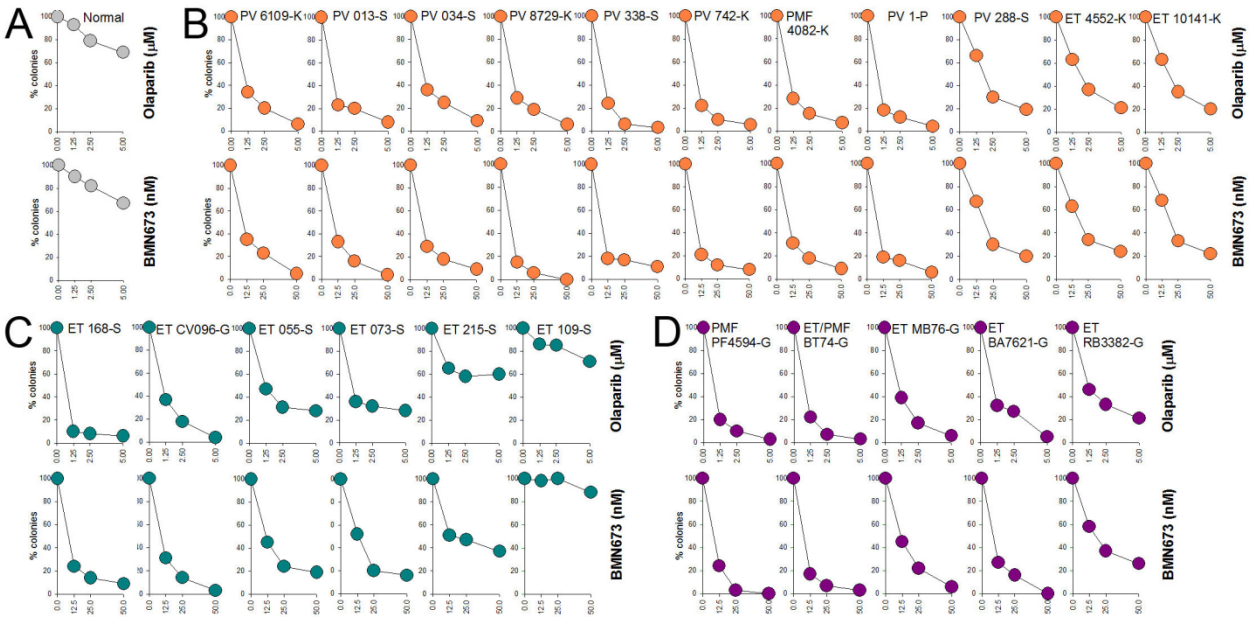

Figure 2

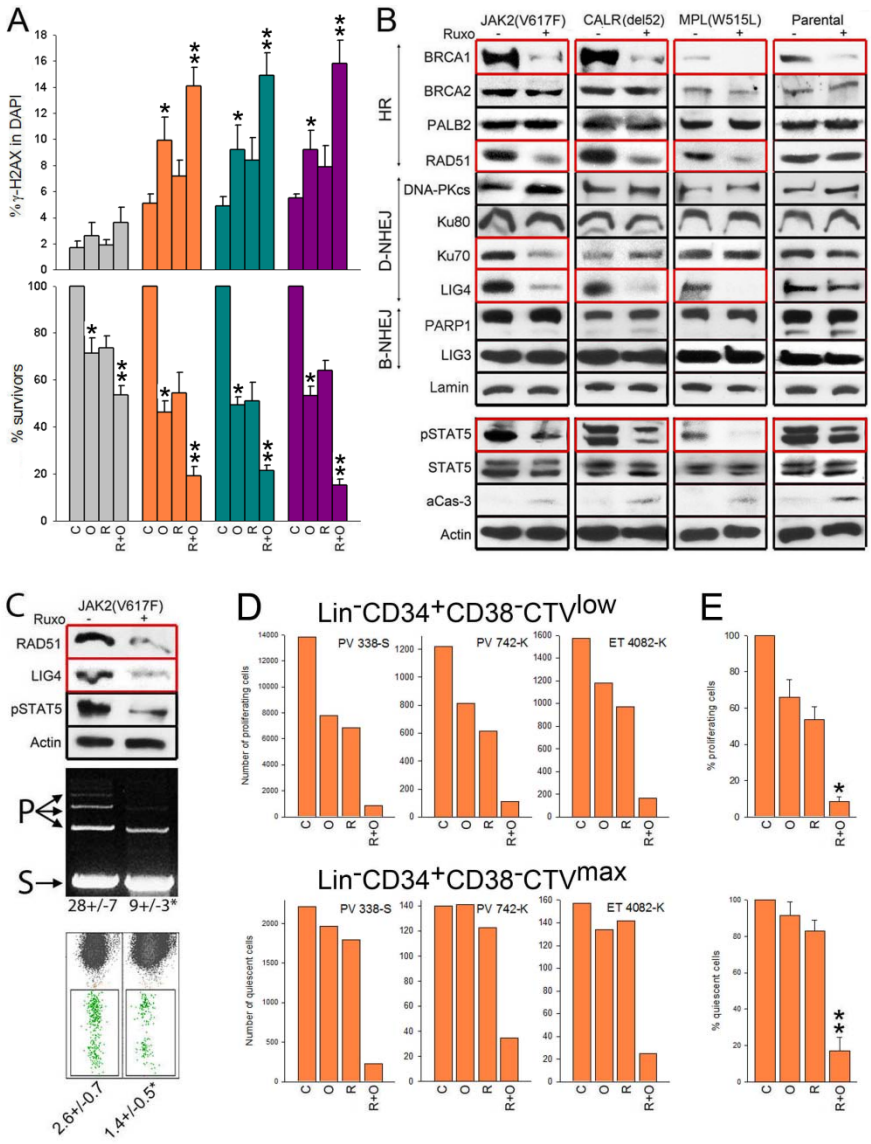
A
% γ-H2AX in DAPI
% survivors
C O R R+O
B
JAK2(V617F)
CALR(del52)
MPL(W515L)
Parental
Ruxo
BRCA1
BRCA2
PALB2
RAD51
DNA-PKcs
Ku80
Ku70
LIG4
PARP1
LIG3
Lamin
HR
D-NHEJ
B-NHEJ
pSTAT5
STAT5
aCas-3
Actin
C
JAK2(V617F)
Ruxo
RAD51
LIG4
pSTAT5
Actin
P
S
28+/-7
9+/-3*
2.6+/-0.7
1.4+/-0.5*
D
Lin-CD34+CD38-CTVlow
PV 338-S
PV 742-K
ET 4082-K
Number of proliferating cells
Lin-CD34+CD38-CTVmax
Number of quiescent cells
E
% proliferating cells
% quiescent cells

Figure 3

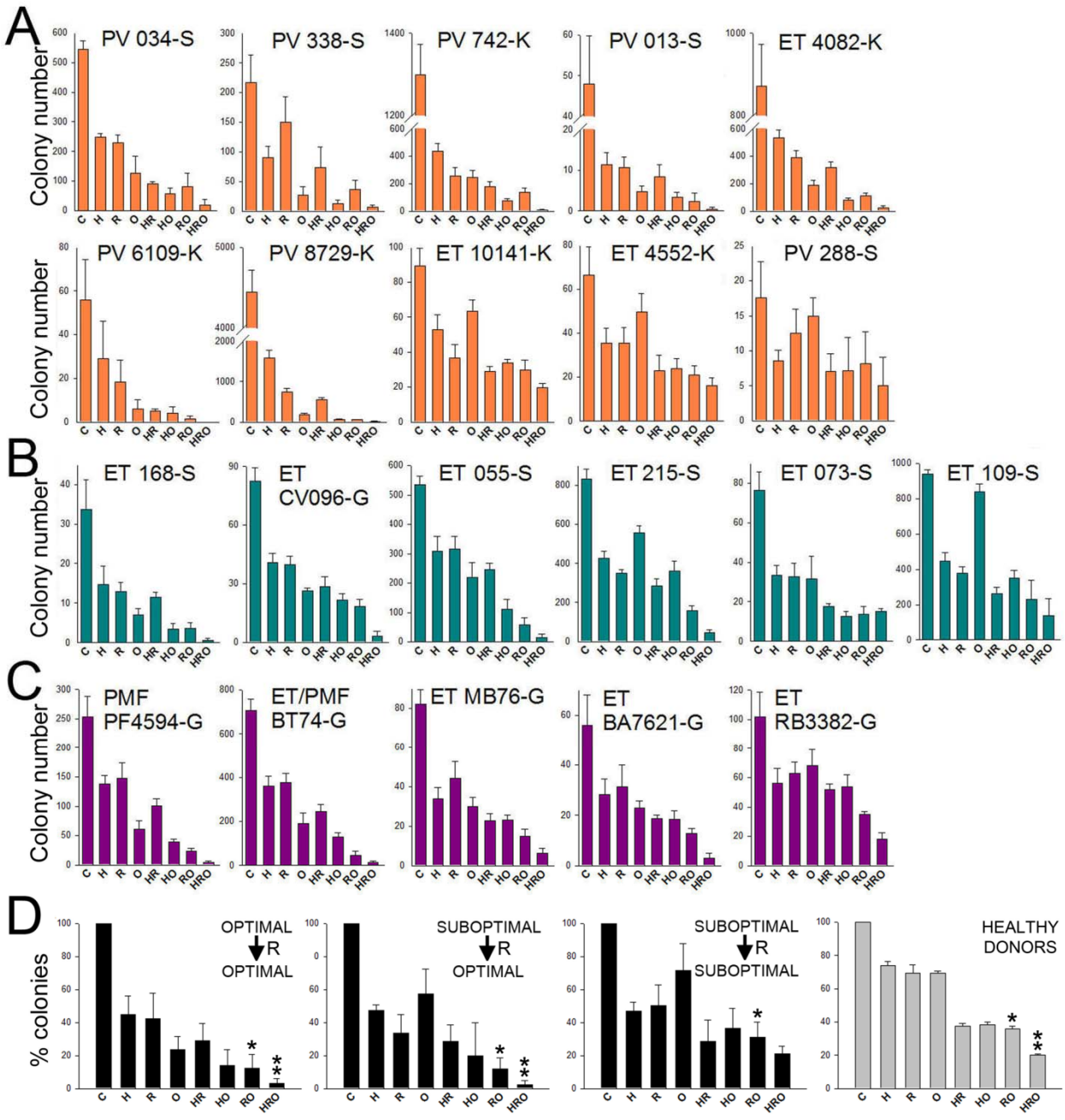
A
Colony number
PV 034-S
PV 338-S
PV 742-K
PV 013-S
ET 4082-K
PV 6109-K
PV 8729-K
ET 10141-K
ET 4552-K
PV 288-S
B
ET 168-S
ET CV096-G
ET 055-S
ET 215-S
ET 073-S
ET 109-S
C
PMF PF4594-G
ET/PMF BT74-G
ET MB76-G
ET BA7621-G
ET RB3382-G
D
% colonies
OPTIMAL R OPTIMAL
SUBOPTIMAL R OPTIMAL
SUBOPTIMAL R SUBOPTIMAL
HEALTHY DONORS
C H R O HR HO RO HRO

Figure 4

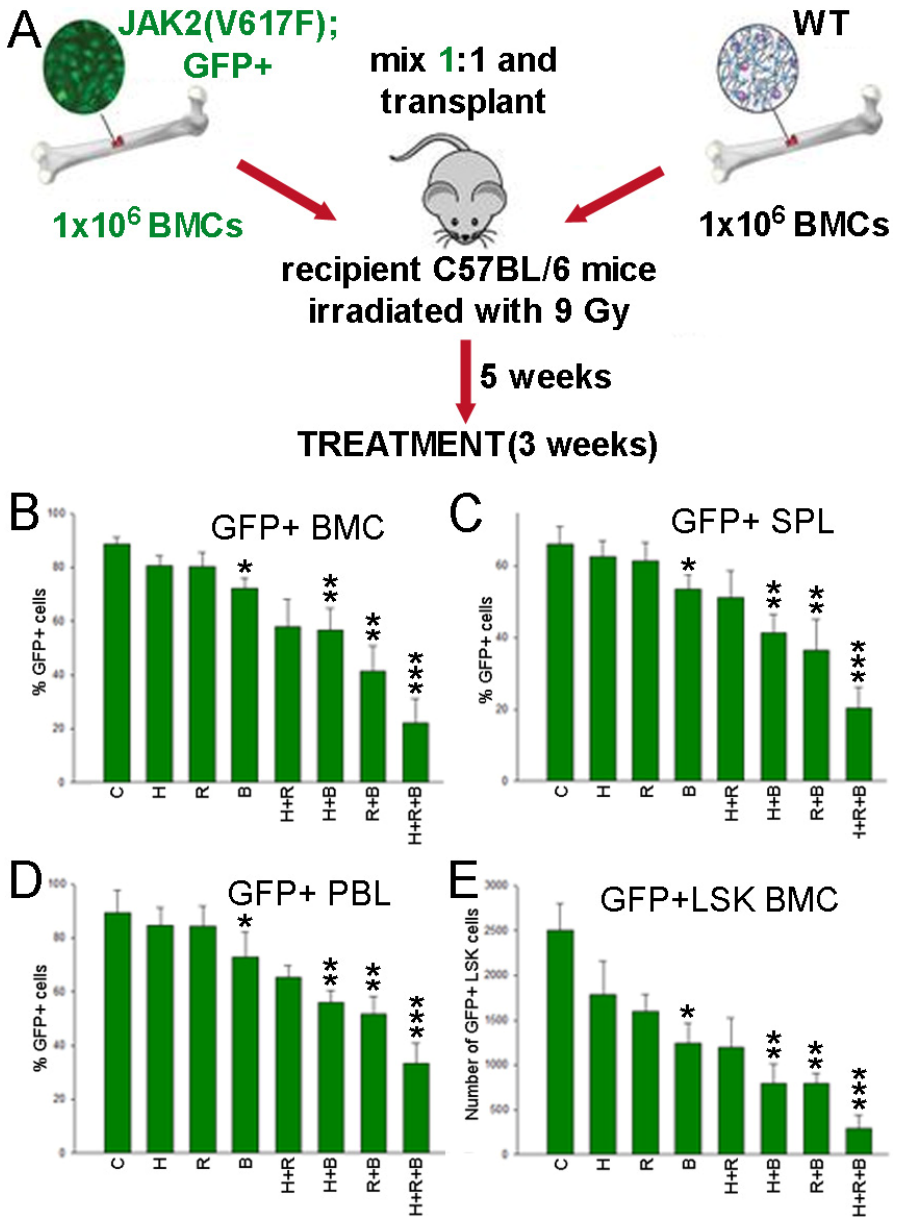
A
JAK2(V617F); GFP+
mix 1:1 and transplant
WT
1x10^6 BMCs
1x10^6 BMCs
recipient C57BL/6 mice irradiated with 9 Gy
5 weeks
TREATMENT(3 weeks)
B
GFP+ BMC
% GFP+ cells
C
GFP+ SPL
% GFP+ cells
D
GFP+ PBL
% GFP+ cells
E
GFP+LSK BMC
Number of GFP+ LSK cells
C
H
R
B
H+R
H+B
R+B
H+R+B

Figure 5

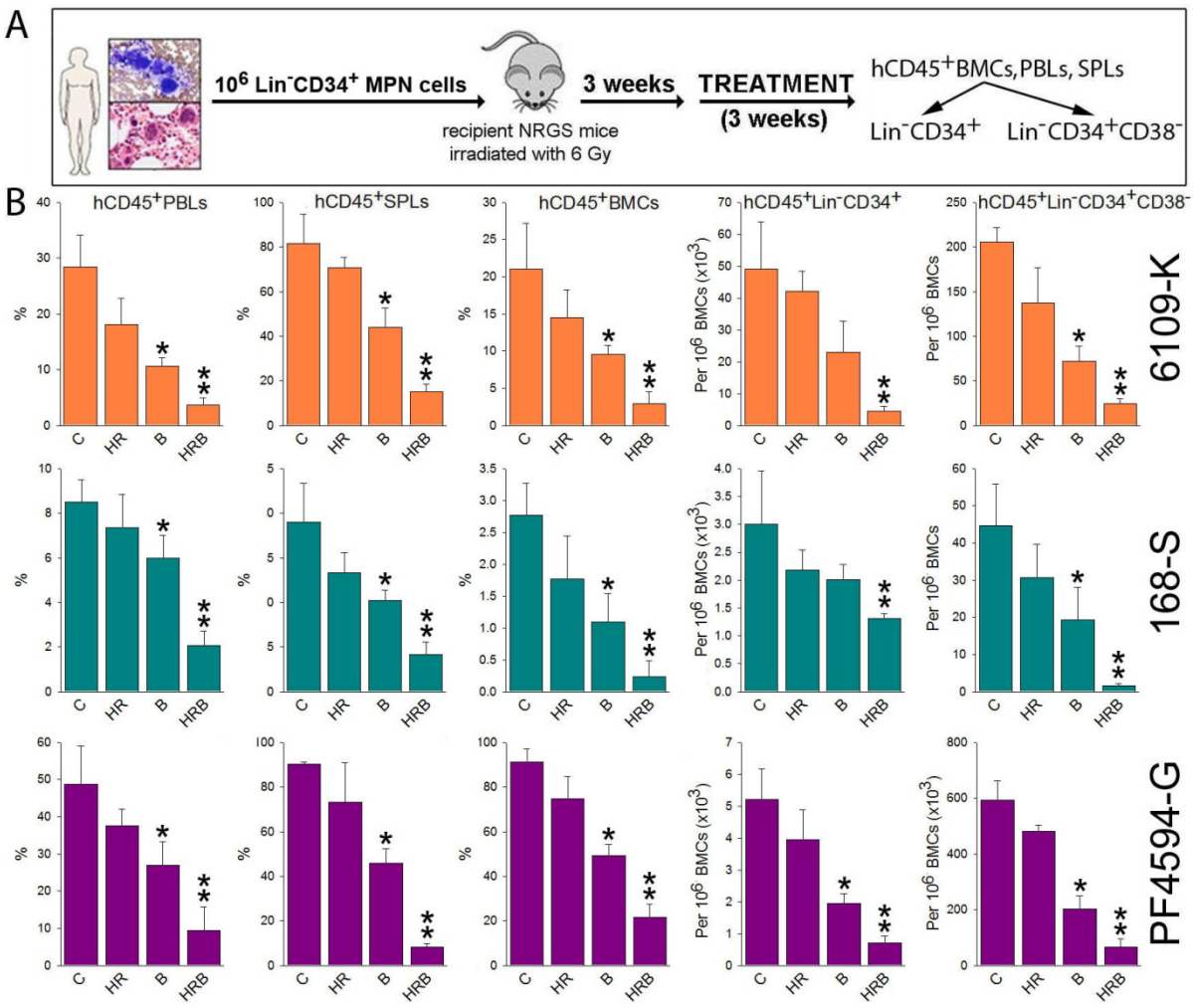
A
10^6 Lin-CD34+ MPN cells
recipient NRGS mice
irradiated with 6 Gy
3 weeks
TREATMENT
(3 weeks)
hCD45+BMCs, PBLs, SPLs
Lin-CD34+
Lin-CD34+CD38-
B
hCD45+PBLs
hCD45+SPLs
hCD45+BMCs
hCD45+Lin-CD34+
hCD45+Lin-CD34+CD38-
%
Per 10^6 BMCs (x10^3)
Per 10^6 BMCs
C
HR
B
HRB
6109-K
168-S
PF4594-G

Figure 6